Patterns of chaos synchronization

Johannes Kestler,[1] Evi Kopelowitz,[2] Ido Kanter,[2] and Wolfgang Kinzel[1]
[1]*Institute for Theoretical Physics, University of Würzburg, Am Hubland, D-97074 Würzburg, Germany*
[2]*Department of Physics, Bar-Ilan University, Ramat-Gan 52900, Israel*
(Received 19 December 2007; published 14 April 2008; publisher error corrected 16 April 2008)

Small networks of chaotic units which are coupled by their time-delayed variables are investigated. In spite of the time delay, the units can synchronize isochronally, i.e., without time shift. Moreover, networks cannot only synchronize completely, but can also split into different synchronized sublattices. These synchronization patterns are stable attractors of the network dynamics. Different networks with their associated behaviors and synchronization patterns are presented. In particular, we investigate sublattice synchronization, symmetry breaking, spreading chaotic motifs, synchronization by restoring symmetry, and cooperative pairwise synchronization of a bipartite tree.

DOI: 10.1103/PhysRevE.77.046209 PACS number(s): 05.45.Xt, 05.45.Ra

I. INTRODUCTION

Chaos synchronization is a counterintuitive phenomenon. On one hand, a chaotic system is unpredictable. Two chaotic systems, starting from almost identical initial states, end in completely different trajectories. On the other hand, two identical chaotic units which are coupled to each other can synchronize to a common chaotic trajectory. The system is still chaotic, but after a transient the two chaotic trajectories are locked to each other [1,2]. This phenomenon has attracted a lot of research activities, partly because chaos synchronization has the potential to be applied for novel secure communication systems [3,4]. In fact, synchronization and bit exchange with chaotic semiconductor lasers has recently been demonstrated over a distance of 120 km in a public fiber-optic communication network [5]. In this case, the coupling between the chaotic lasers was unidirectional, the sender was driving the receiver. For bidirectional couplings, when two chaotic units are interacting, additional interesting applications have been suggested. In this case, a secure communication over a public channel may be established. Although the algorithm as well as all the parameters are public, it is difficult for an attacker to decipher the secret message [6–8].

Typically, the coupling between chaotic units has a time delay due to the transmission of the exchanged signal. Nevertheless, chaotic units can synchronize without time shift, isochronically, although the delay time may be extremely long compared to the time scales of the chaotic units. This—again counterintuitive—phenomenon has recently been demonstrated with chaotic semiconductor lasers [9–12], and it is discussed in the context of corresponding measurements on correlated neural activity [13–16].

Several chaotic units may be coupled to a network with delayed interactions. Such a network can synchronize completely to a single chaotic trajectory, or it may end in a state of several clusters, depending on the topology of the network or the distribution of delay times [17–20]. Recently another phenomenon has been reported for chaotic networks: Sublattice synchronization. If a small network can be decomposed into two sublattices, then the units in each sublattice can synchronize to a common chaotic trajectory although they are not directly coupled. The coupling of one sublattice is relayed by the chaotic trajectory of a different sublattice. The trajectories of different sublattices are only weakly correlated, but not synchronized [21].

In this paper we want to investigate patterns of chaos synchronization for several lattices with uni- and bidirectional couplings with time delay. There exists a mathematical theory to classify possible solutions of nonlinear differential or difference equations for a given lattice [22]. In fact, this theory stimulated us to investigate patterns of sublattice synchronization as discussed in Secs. III and IV. However, this theory does not determine the stability of these solutions. But in order to describe physical or biological dynamic networks, we are interested in *stable* patterns of chaotic networks. The patterns which are discussed in this paper are attractors in phase space, any perturbation of the system will relax to these patterns which move chaotically on some high dimensional synchronization manifold. Throughout our paper, "synchronization" means "stable synchronization."

We present a collection of different results which show new relations and phenomena. Some of these examples show rather unexpected patterns of stable chaos and point to general statements. Our results are demonstrated for iterated maps, for the sake of simplicity and since we can calculate the stability of these networks analytically. But some of our relations are rather general, and some of our results have been seen in other systems by numerical simulations. Thus we believe that our examples contribute to a general understanding of networks of interacting chaotic units.

In particular, in Sec. II we consider the simplest system, two interacting units with delayed couplings. The phase diagram has already been calculated analytically in Ref. [21]. Here we show that this phase diagram of mutually coupled units can be obtained from the phase diagram of a driven unit. This relation is not limited to iterated Bernoulli maps, but it holds, for example, for the Lang-Kobayashi rate equations describing semiconductor lasers as well. This is shown in Sec. VII.

In Sec. III our previous investigations on sublattice synchronization are extended to chaotic units on asymmetric rings and on triangular lattices. Speculations on the symmetry of chaotic patterns are presented. In Sec. IV it is shown that patterns of a small chaotic system can be transmitted to

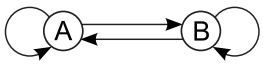

FIG. 1. Two mutually coupled units.

infinitely large lattices with directed delayed couplings. The complete lattice may relax to a pattern of sublattice synchronization, depending on the coupling strength. The symmetry of a lattice determines the structure of synchronization patterns. This is demonstrated for chains with four and five units in Sec. V. Finally, in Sec. VI a different phenomenon is presented: cooperative pairwise synchronization of a bipartite tree coupled by a single channel. Section VIII summarizes the results of this paper.

II. TWO INTERACTING UNITS

We start with the simplest network: two units with delayed couplings and delayed self-feedback, as sketched in Fig. 1. For iterated maps, this network is described by the following equations:

$$a_t = (1-\varepsilon)f(a_{t-1}) + \varepsilon\kappa f(a_{t-\tau}) + \varepsilon(1-\kappa)f(b_{t-\tau}),$$

$$b_t = (1-\varepsilon)f(b_{t-1}) + \varepsilon\kappa f(b_{t-\tau}) + \varepsilon(1-\kappa)f(a_{t-\tau}), \qquad (1)$$

where $f(x)$ is some chaotic map, for example the Bernoulli shift,

$$f(x) = \alpha x \bmod 1 \qquad (2)$$

with $\alpha > 1$. In this case, the system is chaotic for all parameters $0 < \varepsilon < 1$ and $0 < \kappa < 1$. ε measures the total strength of the delay terms and κ the strength of the self-feedback relative to the delayed coupling.

Obviously, the synchronized chaotic trajectory $a_t = b_t$ is a solution of Eq. (1). Its stability is determined by τ conditional Lyapunov exponents which describe the stability of perturbations perpendicular to the synchronization manifold. For the Bernoulli map, these Lyapunov exponents have been calculated analytically [21,23], and for infinitely long delay, $\tau \to \infty$, one obtains the phase diagram of Fig. 2.

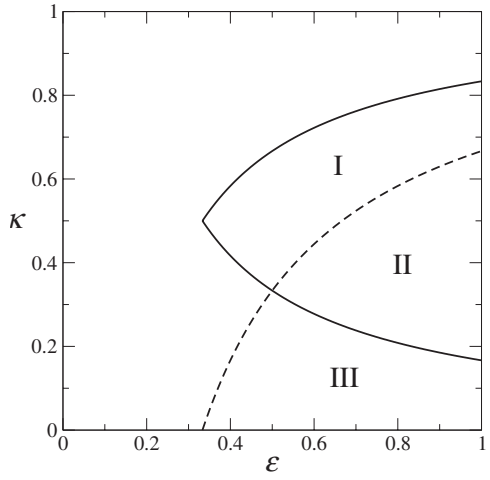

FIG. 2. Phase diagram for $\alpha = 3/2$ (analytical result).

In regions I and II, i.e., for

$$\frac{\alpha - 1}{2\alpha\varepsilon} < \kappa < \frac{2\alpha\varepsilon + 1 - \alpha}{2\alpha\varepsilon}, \qquad (3)$$

the two units are synchronized to an identical chaotic trajectory $a_t = b_t$. Although the two units are coupled with a long delay τ, they are completely synchronized without any time shift. For $\tau \to \infty$, this region is symmetric about the line $\kappa = \frac{1}{2}$. Typically, already a delay time of $\tau = 50$ is sufficient to resemble the analytic results for $\tau \to \infty$, i.e., the region of synchronization approximates the analytic result shown in Fig. 2. For smaller delay times τ, the region of synchronization (I and II) changes and is not symmetric around the line $\kappa = \frac{1}{2}$.

Complete synchronization can be understood by considering a single unit driven by some signal s_t:

$$a_t = (1-\varepsilon)f(a_{t-1}) + \varepsilon\tilde{\kappa}f(a_{t-\tau}) + s_{t-\tau}. \qquad (4)$$

If the system is not chaotic, i.e., if its Lyapunov exponents are negative, then the trajectory a_t relaxes to a unique trajectory determined by the drive s_t. For the Bernoulli shift, this region is defined by the inequality (for $\tau \to \infty$)

$$\left(-\frac{1 + \alpha\varepsilon - \alpha}{\alpha\varepsilon} <\right) \tilde{\kappa} < \frac{1 + \alpha\varepsilon - \alpha}{\alpha\varepsilon} \qquad (5)$$

and indicated by II+III in Fig. 2. Since the trajectory which A relaxes to is uniquely determined by the drive, further identical units receiving the same drive would relax to the same trajectory. Thus Eq. (5) defines the region where identical units which get the same input synchronize to a common trajectory.

Now let us rewrite Eq. (1):

$$a_t = (1-\varepsilon)f(a_{t-1}) + \varepsilon(2\kappa - 1)f(a_{t-\tau}) + \varepsilon(1-\kappa)f(a_{t-\tau}) + \varepsilon(1-\kappa)f(b_{t-\tau}),$$

$$b_t = (1-\varepsilon)f(b_{t-1}) + \varepsilon(2\kappa - 1)f(b_{t-\tau}) + \varepsilon(1-\kappa)f(b_{t-\tau}) + \varepsilon(1-\kappa)f(a_{t-\tau}). \qquad (6)$$

Both systems are driven by the identical signal

$$s_{t-\tau} = \varepsilon(1-\kappa)[f(a_{t-\tau}) + f(b_{t-\tau})]. \qquad (7)$$

Comparing Eq. (4) with Eq. (6), one finds that for

$$\tilde{\kappa} = 2\kappa - 1 \qquad (8)$$

the interacting units (6) are described by the driven unit (4). The phase boundary of the driven system, region II+III [Eq. (5)], and the phase boundary of the interacting system, region I+II [Eq. (3)], are connected with each other: With the mapping of Eq. (8), one phase boundary can be obtained from the other. This is not only true for $\tau \to \infty$ but for any value of τ.

Additionally, this mapping does not only hold for the Bernoulli shift but for any chaotic system, provided that the signal does not change the Lyapunov exponents of the driven system. Simulations with other maps, e.g., with the tent map or the logistic map, confirm the applicability of the mapping (8). Since the slopes of these maps are not constant, the

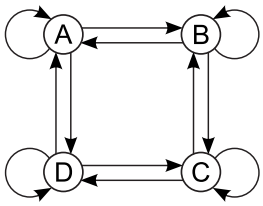

FIG. 3. Ring of four units.

Lyapunov exponents depend on the trajectories; in order to get trajectories which are comparable to the trajectories of two mutually coupled units, the driving signal in the driver-receiver setup must come from an identical unit c_t (which has an increased self-coupling due to the lack of external couplings), i.e.,

$$s_{t-\tau} = \varepsilon(1-\tilde{\kappa})f(c_{t-\tau}) \tag{9}$$

with

$$c_t = (1-\varepsilon)f(c_{t-1}) + \varepsilon f(c_{t-\tau}). \tag{10}$$

Even for the Lang-Kobayashi equations [24,25], which describe coupled semiconductor lasers, we found a good agreement for the mapping (8); see Sec. VII.

Now let us come back to the iterated Eqs. (1). Let us assume that we record the synchronized trajectory $a_t = b_t$ of two interacting chaotic units, regions I and II of Fig. 2. Now we insert the recorded trajectory b_t into Eq. (1). How will a_t respond to this drive? We find that in region II the unit A will synchronize completely to the recorded trajectory b_t, whereas in region I the unit A does not synchronize. Although the two interacting units A and B do synchronize, the unit A does not follow the recorded trajectory in region I. This shows that bidirectional interaction is different from unidirectional drive.

III. SUBLATTICE SYNCHRONIZATION

The response of a single chaotic unit to an external drive, Fig. 2, determines also the phase diagram of a ring of four chaotic units. Additionally, it shows an interesting phenomenon: sublattice synchronization [21]. Consider the ring of four identical units of Fig. 3. The dynamics of unit A is described by

$$a_t = (1-\varepsilon)f(a_{t-1}) + \varepsilon\kappa f(a_{t-\tau}) + \varepsilon(1-\kappa)\left[\frac{1}{2}f(b_{t-\tau}) + \frac{1}{2}f(d_{t-\tau})\right]; \tag{11}$$

the dynamics of B, C, and D are defined analogously. Note the additional weight $\frac{1}{2}$ for the external coupling (to two neighbors) which causes the total strength of the external coupling to remain $\varepsilon(1-\kappa)$.

Obviously, the two units A and C receive identical input from the units B and D. Consequently, they will respond with an identical trajectory in regions II and III of Fig. 2. The same argument holds for the two units B and D, which both get the same input from A and C. That leads to sublattice synchronization in region III of Fig. 2: A and C have an identical chaotic trajectory and B and D have a different one. Although there is a delay of arbitrary long time of the transmitted signal, synchronization is complete, without any time shift. The synchronization of A and C is mediated by the chaotic trajectory of B and D and vice versa. But the two trajectories have only weak correlations, they are not synchronized. Numerical simulations of the Bernoulli system with small values of τ have shown that there is no generalized synchronization either [21,26,27].

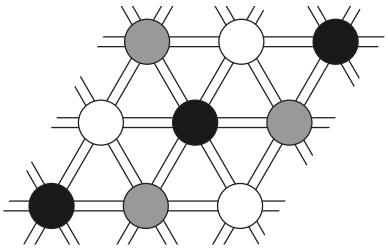

FIG. 4. Sublattice synchronization in a triangular lattice with periodic boundaries. The double lines signify bidirectional couplings. The self-feedback is not drawn to simplify the illustration.

Sublattice synchronization has been found for rings with an even number of units, for chains and also for other lattices which can be decomposed into identical sublattices [21]. The corresponding equations for a general lattice are

$$x_t^j = (1-\varepsilon)f(x_{t-1}^j) + \varepsilon\kappa f(x_{t-\tau}^j) + \varepsilon(1-\kappa)\sum_k F_{j,k} f(x_{t-\tau}^k), \tag{12}$$

where $F_{j,k}$ is the weighted adjacency matrix which has (usually) a component $1/z_j$ if unit j is coupled to node k and 0 otherwise, and z_j is the number of connections to unit j.

For example, the lattice of Fig. 4 can be decomposed into three sublattices. For some parameters of the Bernoulli system we find sublattice synchronization with three chaotic trajectories. Again, the synchronized units are not directly coupled, but they are indirectly connected via the trajectories of the other sublattices.

The sublattice trajectories, described before, are stable, i.e., the conditional Lyapunov exponents which describe perturbations perpendicular to the synchronization manifold are negative. Even when the system starts from random initial states it relaxes to the state of sublattice synchronization (region III of Fig. 2 for the ring of four units). The chaotic trajectories of sublattice synchronization may be depicted as $\begin{smallmatrix} A & B \\ B & A \end{smallmatrix}$. Note that this structure does not break the symmetry of the ring: the statistical properties of the chaotic trajectory of A are identical to those of B.

However, there are other solutions of the dynamic equations, as well. These solutions are classified according to the theory of Golubitsky *et al.* [22]. For example, for the ring, the state $\begin{smallmatrix} A & B \\ A & B \end{smallmatrix}$ is a solution as well. Such a state breaks the symmetry of the lattice. But we find that this state is unstable. Any tiny perturbation relaxes to the states $\begin{smallmatrix} A & B \\ B & A \end{smallmatrix}$ in region III, $\begin{smallmatrix} A & A \\ A & A \end{smallmatrix}$ in region II, and $\begin{smallmatrix} A & B \\ D & C \end{smallmatrix}$ outside of II and III. In fact, we have never found a stable state which breaks the symmetry of the lattice. Only when the couplings in the two direc-

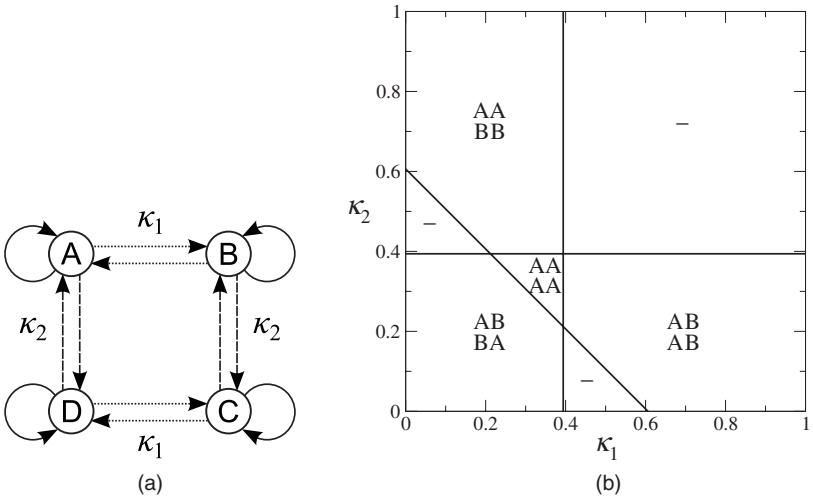

FIG. 5. Ring of four units with two different coupling parameters κ_1 and κ_2. (a) Illustration of the setup. (b) Phase diagram for Bernoulli system with $\alpha=3/2$ and $\varepsilon=11/20$ (analytical result). The regions of no synchronization are labeled with a dash (–).

tions of the ring are different, the states $\begin{smallmatrix} A & B \\ A & B \end{smallmatrix}$ and $\begin{smallmatrix} A & A \\ B & B \end{smallmatrix}$ are stable in some (different) parts of the parameter space; see Fig. 5. Hence we postulate that spontaneous symmetry breaking is not possible for finite lattices of chaotic units. We are not able to prove this statement, but we have not found any counterexample yet.

IV. SPREADING CHAOTIC MOTIFS

The response of a chaotic unit to an external drive, Fig. 2, points to another interesting phenomenon. Consider a triangle of chaotic units with bidirectional couplings as sketched in Fig. 6(a). The equations correspond to Eq. (12). Choose the parameters such that the triangle is completely disordered, but each unit has negative Lyapunov exponents when it is separated from the two others. [Both conditions are fulfilled in region III of Fig. 6(b), which shows analytical results for the Bernoulli system.] When we record the three time series a_t, b_t, and c_t we find three different weakly correlated chaotic trajectories. Now we feed the two trajectories b_t and c_t into an infinitely large lattice of identical units with unidirectional couplings as shown in Fig. 6(a). Each unit receives two input signals from two other units. But since all Lyapunov exponents are negative, the system responds with the three chaotic trajectories a_t, b_t, and c_t. Although the units of the initial triangle are not synchronized, their pattern of chaos is transmitted to the infinite lattice. All units of the same sublattice are completely synchronized without time shift, although the coupling has a long delay time τ. Hence the chaotic motif, three weakly correlated chaotic trajectories, can be imposed on an arbitrarily large lattice. Note that the time for spreading a motif on a large lattice increases only linearly with the number of units because of the unidirectional couplings.

For some parameters κ and ε, namely in regions I and II of Fig. 6(b), the three units of the triangle are completely synchronized. In region I, only the three units are synchro-

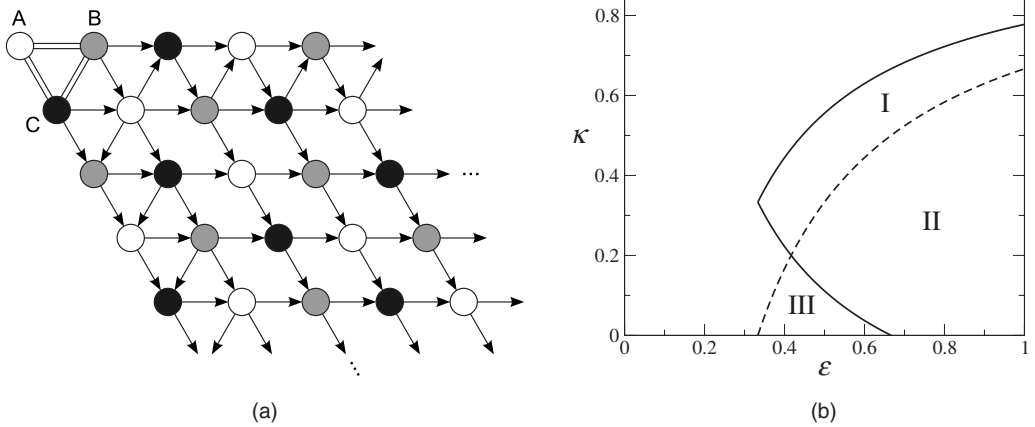

FIG. 6. Triangle (three bidirectionally coupled units) with a unidirectionally attached infinitely large lattice. (a) Double lines signify bidirectional couplings whereas arrows show unidirectional couplings. The self-feedback is not drawn to simplify the illustration. The colors indicate the synchronization pattern (sublattice synchronization) of region III. (b) Phase diagram for Bernoulli system, $\alpha=3/2$. Analytical result combining (1) the analytical synchronization region for a ring of three units (—) and (2) the region where identical units which are driven by an identical signal synchronize (– –).

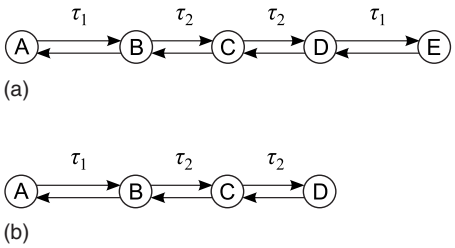

FIG. 7. Symmetric (a) and asymmetric (b) chain without self-feedback and with two different time delays.

nized while the other units remain unsynchronized. In region II, the other units, too, get synchronized to the triangle (because all Lyapunov exponents are negative), so the whole lattice is completely synchronized.

The phenomenon of spreading motifs is not restricted to a triangle. For example, a ring of six mutually coupled units has also a region in the corresponding (ε,κ) phase diagram where there is no synchronization, but where isolated units have negative Lyapunov exponents, comparable to region III in Fig. 6(b) [21]. Consequently, the pattern of six chaotic trajectories can lead to sublattice synchronization with six different sublattices on a corresponding lattice of chaotic units with short-range unidirectional couplings.

Again, we want to emphasize that these results are not based on numerical simulations, but they are analytic results obtained from calculating the spectrum of transverse Lyapunov exponents [21]. Of course, we have checked these results by numerical simulations.

V. SYNCHRONIZATION BY RESTORING SYMMETRY

In general we expect that the larger the network is, the smaller the region in the parameter space is where the network synchronizes. For example, a ring of $N=6$ units has a smaller region of synchronization than regions II and III of Fig. 2 for $N=4$. With increasing N (and the slope α being held constant) synchronization finally disappears completely [21]. However, we found a counterexample where adding a unit restores synchronization.

Consider the chain of five units shown in Fig. 7(a) with a dynamics corresponding to Eq. (12), where the coupling to the two outer units has a longer delay time than the internal couplings, and there is no self-feedback, $\kappa=0$. Now remove unit E, Fig. 7(b), and rescale the coupling to unit D. (Unit D doubles the input from unit C to compensate for the missing second neighbor.) In this case, a synchronized solution does not exist. Numerical simulations of the Bernoulli system and the laser equations show high correlations between units A and C with time shift $\Delta=\tau_1-\tau_2$, and between B and D with zero time shift, but the correlation coefficient does not achieve the value one. On the other side, if we add unit E we restore the symmetry of the chain. In this case we find sublattice synchronization with time shift between the outer units and the central one:

$$a_t = e_t = c_{t-\Delta}; \quad b_t = d_t. \tag{13}$$

If τ_1 is greater than τ_2, the central unit is earlier than the chaotic trajectory of the outer ones, it leads, whereas for the opposite case it lags behind.

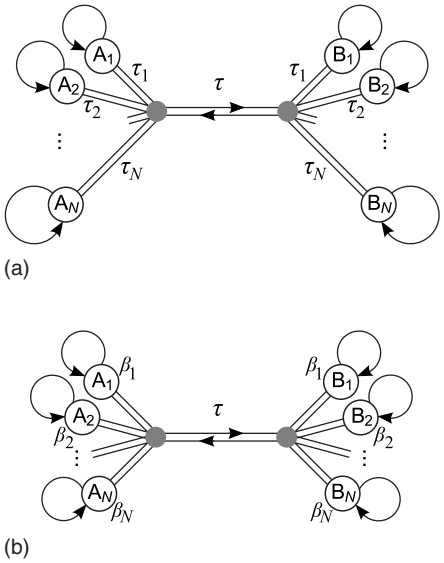

FIG. 8. Setups where each unit on one side is coupled to all units of the other side. (a) There are N different delay times which are pairwise identical for one unit of side A and one unit of side B. (b) There are N different shifts in the Bernoulli map which are pairwise identical for one unit of side A and one unit of side B. The shaded dots indicate that the signals of each side of the tree are summed up and a single signal is transmitted to the other side and there distributed (second shaded dot) among the units.

VI. COOPERATIVE PAIRWISE SYNCHRONIZATION

Is it possible to synchronize two sets of chaotic units with a single coupling channel? In fact, we found such examples where two sets of chaotic units are bidirectionally connected by the sum of their units, as indicated in Fig. 8. There are $2N$ units, i.e., the number of units on each side is N. Each side is the mirror image of the other. Only one single bidirectional signal composed of all N signals from each side is driving the other side, and this leads to cooperative pairwise synchronization.

In the first setup, Fig. 8(a), all units are identical, but the delay times of their couplings are different. The units have pairwise identical delay times, i.e., A_k and B_k have a coupling delay time $2\tau_k+\tau$ which is enforced by a self-feedback with delay time $\tau_s=2\tau_k+\tau$. Hence for one pair, $N=1$, we obtain the phase diagram of Fig. 2, where the two units are completely synchronized in regions I and II. For a large number N of units, a unit A_j receives the signal

$$s_{j,t} = \varepsilon(1-\kappa)\frac{1}{N}\sum_{k=1}^{N} f(b_{k,t-(\tau_j+\tau_k+\tau)}) \tag{14}$$

and vice versa. Note that the signals $s_{j,t}$ for different j are only time shifted by τ_j; only one common signal (for each direction) has to be transmitted over the channel. Note also that a unit A_k receives only a weak signal of the order $1/N$ from its counterpart B_k. Nevertheless, we find that the network synchronizes to a state of pairwise identical chaotic trajectories, $a_{k,t}=b_{k,t}; k=1,\ldots,N$. For the Bernoulli system, the region of pairwise synchronization is similar to region II of Fig. 2. There is no synchronization among units of the

same side. Each unit receives the sum of all chaotic trajectories, but it responds only to the tiny part which belongs to its counterpart. The synchronization is a cooperative effect. As soon as a single unit is detuned, the whole network loses synchronization.

The second setup, Fig. 8(b), is similar to the first one but allows analytical calculations. In this second setup, all delay times are identical, while each unit of one side has a different shift β_k, $k=1,\ldots,N$, in its shifted Bernoulli map, see Eq. (15); the shifts are pairwise identical for unit A_k and the corresponding unit B_k so one side is again the mirror image of the other side. The shifted Bernoulli map is defined by

$$f_\beta(x) = [\alpha(x+\beta)] \bmod 1. \tag{15}$$

Each A unit receives the signal

$$s_t = \varepsilon(1-\kappa)\frac{1}{N}\sum_{k=1}^{N} f_{\beta_k}(b_{k,t-\tau}) \tag{16}$$

and vice versa. Analytical calculations are possible for this second setup because the delay times are equal—in contrast to the first setup—and the different shifts in the map do not hamper the calculations. If the Bernoulli maps were not shifted, the units would all be identical. Then in regions II and III of Fig. 2, all units of the same side would synchronize, $a_{1,t}=a_{2,t}=\cdots=a_{N,t}$; $b_{1,t}=b_{2,t}=\cdots=b_{N,t}$ because they receive the same input. Then one would effectively get two coupled units A and B (which synchronize in regions I and II), so in region II all $2N$ units would be synchronized. For *shifted* Bernoulli maps, the units of the same side are not allowed to synchronize by definition. Nevertheless, the stability analysis regarding the linearized equations is not affected by the different shifts, meaning that the same perturbations still are damped in the same regions; the only difference is that due to the shifts, most of the trajectories are not allowed to come close together. Only the pairs of corresponding units can synchronize, $a_{k,t}=b_{k,t}$, and so they do in region II.

VII. ANALOGY OF LASER EQUATIONS TO ITERATED MAPS

Besides iterated maps, we considered the Lang-Kobayashi equations, which describe the dynamics of semiconductor lasers optically coupled to their own or/and to the light of other semiconductor lasers. We used them for simulations in the following form, according to Ref. [25]:

$$\begin{aligned}\frac{d}{dt}E_{0,j}(t) = {} & \frac{1}{2}G_N n_j(t)E_{0,j}(t) + \frac{C_{\mathrm{sp}}\gamma[N_{\mathrm{Sol}}+n_j(t)]}{2E_{0,j}(t)} \\ & + \lambda E_{0,j}(t-\tau)\cos[\omega_0\tau+\phi_j(t)-\phi_j(t-\tau)] \\ & + \sigma\sum_{k=1}^{N_{\mathrm{lasers}}} w_{j,k}E_{0,k}(t-\tau) \\ & \times\cos[\omega_0\tau+\phi_j(t)-\phi_k(t-\tau)],\end{aligned} \tag{17}$$

$$\begin{aligned}\frac{d}{dt}\phi_j(t) = {} & \frac{1}{2}\alpha_{\mathrm{lef}}G_N n_j(t) - \lambda\frac{E_{0,j}(t-\tau)}{E_{0,j}(t)}\sin[\omega_0\tau+\phi_j(t) \\ & -\phi_j(t-\tau)] - \sigma\sum_{k=1}^{N_{\mathrm{lasers}}} w_{j,k}\frac{E_{0,k}(t-\tau)}{E_{0,j}(t)} \\ & \times\sin[\omega_0\tau+\phi_j(t)-\phi_k(t-\tau)],\end{aligned} \tag{18}$$

$$\frac{d}{dt}n_j(t) = (p-1)\gamma N_{\mathrm{sol}} - \gamma n_j(t) - [\Gamma + G_N n_j(t)]E_{0,j}^2(t), \tag{19}$$

where $E_{0,j}(t)$ and $\phi_j(t)$ are the amplitude and the slowly varying phase of the electric field $E_j(t)=E_{0,j}(t)\exp\{i[\omega_0\tau+\phi_j(t)]\}$ and $n_j(t)$ is the carrier number above the value for a solitary laser, $j=1,\ldots,N_{\mathrm{lasers}}$. The strength of the self-feedback is determined by λ, while the strength of the external coupling is defined by σ. The equations above cover the general case of N_{lasers} coupled semiconductor lasers, where the network structure and coupling strengths are determined by the weightings $w_{j,k}$, which are normalized so that the strength of the total input for each laser is the same, $\Sigma_{k=1}^{N_{\mathrm{lasers}}}w_{j,k}=1$ for each laser j [28]. The parameters N_{sol}, G_N, τ, α_{lef}, γ, Γ, p, ω_0, and C_{sp} are chosen according to Ref. [25].

In a very simplified form, the equations above read

$$\begin{aligned}\frac{d}{dt}x = {} & [\text{internal dynamics}] + \lambda[\text{self-feedback}] \\ & + \sigma[\text{external coupling}].\end{aligned} \tag{20}$$

Comparing Eqs. (1) and (20) yields a relation between the parameter space of the Lang-Kobayashi equations, $\{\lambda,\sigma\}$, and the parameter space of the maps, $\{\varepsilon,\kappa\}$, if the two following conditions are considered: (i) The ratio of the self-feedback to the external coupling should be the same in both cases. (ii) The ratio of the time-delayed terms to the internal dynamics should be the same in both cases. These two conditions yield the following transformation:

$$\kappa = \frac{\lambda}{\lambda+\sigma}, \quad \varepsilon = \frac{\lambda+\sigma}{v}. \tag{21}$$

The second condition (ii) is not properly defined because the Lang-Kobayashi Eqs. (20)—in contrast to the iterated Eqs. (1)—are differential equations and the internal dynamics is not only the first term on the right-hand side of Eq. (20) but is also contained in the current state x. Therefore the denominator v in Eq. (21) is not given and has to be chosen reasonably. We took $v=180\ \mathrm{ns}^{-1}$ so ε is between 0 and 1 [because the sum $\lambda+\sigma$ (the strength of the re-injected light) should not exceed the value of $v=180\ \mathrm{ns}^{-1}$ in our case].

In order to measure synchronization, we averaged the amplitudes of the electric fields, $E_{0,j}$, in 1 ns intervals and calculated the unshifted, $\Delta=0$, cross correlation function defined by

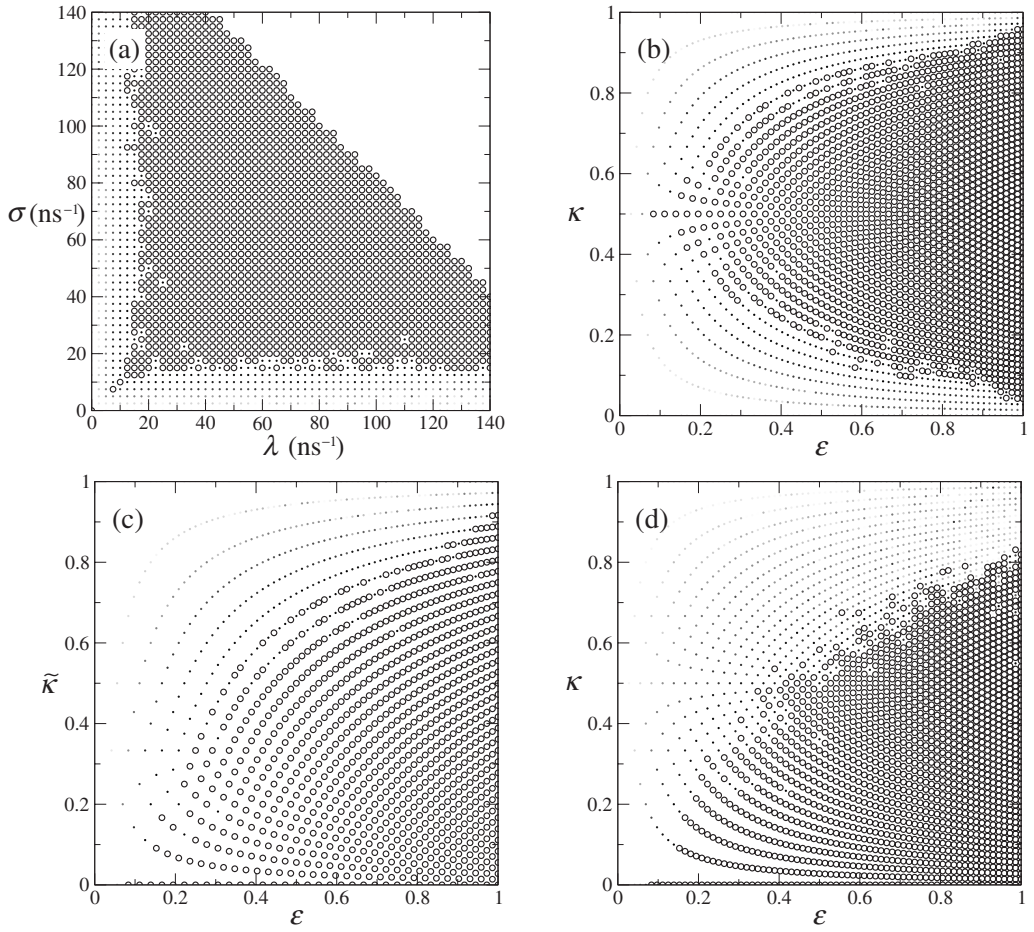

FIG. 9. Phase diagrams for the Lang-Kobayashi laser equations. Every circle or point represents one simulation. Open circles (○) show a cross correlation $C>0.99$, which can be regarded as synchronization in the case of the laser equations. Figure (a) shows results for two mutually coupled lasers, $A \rightleftarrows B$, before applying transformation (21), whereas (b) shows the same diagram after the parameter transformation. The synchronization region of two mutually coupled units (b) can be mapped [using Eq. (8)] to a region (c) which is similar to the synchronization region of a driver-receiver system (d), $A' \leftarrow S \rightarrow A$. After the parameter transformation (21), the synchronization regions for the Lang-Kobayashi equations, (b), (c), and (d), look very similar to the ones for the Bernoulli maps, Fig. 2.

$$C_{xy}^{\Delta} = \frac{\langle x_t y_{t-\Delta}\rangle - \langle x\rangle\langle y\rangle}{\sqrt{\langle x^2\rangle - \langle x\rangle^2}\sqrt{\langle y^2\rangle - \langle y\rangle^2}}. \tag{22}$$

A cross correlation over 0.99 can be regarded as synchronization in the case of lasers.

Figure 9 shows both the parameter transformation, Eq. (21), from $\{\lambda, \sigma\}$ to $\{\varepsilon, \kappa\}$ and the mapping, Eq. (8), from two mutually coupled units to driven ones. From the comparison of this figure with Fig. 2, the analogy of laser equations to iterated maps can be seen. Besides the analogy of features described in Sec. II, one can also find this analogy for the features described in Secs. III, V, and VI.

VIII. SUMMARY

Small networks of chaotic units with time-delayed couplings show interesting patterns of chaos synchrony. These patterns are stable attractors of the network dynamics.

A collection of several lattices is investigated which show new and unexpected kinds of chaotic patterns. Surprisingly, some of these complex patterns can already be understood in terms of a single driven unit, given by the phase diagram of Fig. 2.

The phase diagram of two and four units with mutual couplings has been related to the properties of a single driven chaotic unit. Two interacting units with self-feedback can synchronize completely, without time shift, even if the delay time is extremely large. When the chaotic trajectory of two interacting units is recorded and used to drive a single identical unit, it turns out that the driven unit synchronizes only in a small part of the phase diagram. Hence interaction is different from drive.

Sublattice synchronization is found for lattices which can be decomposed into a few sublattices. Each sublattice is completely synchronized, but different sublattices are only weakly correlated. Synchronization is relayed by different chaotic trajectories. The trajectories of each sublattice have identical statistical properties. Thus the symmetry of the lattice is not broken. There are solutions of the dynamic equations which break the symmetry of the lattice. However, we always found that these solutions are unstable. Hence we postulate that stable patterns of chaos synchrony possess the symmetry of the corresponding lattice. We are not able to

prove this statement, but we have not found any counterexample yet. Synchronization depends on the symmetry of the network. When the symmetry of an asymmetric chain is restored by adding units, sublattice or complete synchronization is restored, too.

Finally, a bipartite network, where the two parts are coupled by a single mutual signal, shows pairwise complete synchronization, whereas the units of each part do not synchronize. Each unit responds to the weak contribution of its partner in the other part of the network. Pairwise synchronization is a cooperative effect: Detuning a single unit destroys the synchronization of the whole network.

ACKNOWLEDGMENT

The work of Ido Kanter was partially supported by the Israel Science Foundation.

[1] A. Pikovsky, M. Rosenblum, and J. Kurths, *Synchronization, A Universal Concept in Nonlinear Sciences* (Cambridge University Press, Cambridge, England, 2001).
[2] H. G. Schuster and W. Just, *Deterministic Chaos* (Wiley VCH, Weinheim, 2005).
[3] L. M. Pecora and T. L. Carroll, Phys. Rev. Lett. **64**, 821 (1990).
[4] K. M. Cuomo and A. V. Oppenheim, Phys. Rev. Lett. **71**, 65 (1993).
[5] A. Argyris, D. Syvridis, L. Larger, V. Annovazzi-Lodi, P. Colet, I. Fischer, J. García-Ojalvo, C. R. Mirasso, L. Pesquera, and K. A. Shore, Nature (London) **438**, 343 (2005).
[6] E. Klein, N. Gross, E. Kopelowitz, M. Rosenbluh, L. Khaykovich, W. Kinzel, and I. Kanter, Phys. Rev. E **74**, 046201 (2006).
[7] E. Klein, R. Mislovaty, I. Kanter, and W. Kinzel, Phys. Rev. E **72**, 016214 (2005).
[8] I. Kanter, N. Gross, E. Klein, E. Kopelowitz, P. Yoskovits, L. Khaykovich, W. Kinzel, and M. Rosenbluh, Phys. Rev. Lett. **98**, 154101 (2007).
[9] E. Klein, N. Gross, M. Rosenbluh, W. Kinzel, L. Khaykovich, and I. Kanter, Phys. Rev. E **73**, 066214 (2006).
[10] I. Fischer, R. Vicente, J. M. Buldu, M. Peil, C. R. Mirasso, M. C. Torrent, and J. García-Ojalvo, Phys. Rev. Lett. **97**, 123902 (2006).
[11] S. Sivaprakasam, J. Paul, P. S. Spencer, P. Rees, and K. A. Shore, Opt. Lett. **28**, 1397 (2003).
[12] M. W. Lee, J. Paul, C. Masoller, and K. A. Shore, J. Opt. Soc. Am. B **23**, 846 (2006).
[13] A. Cho, Science **314**, 37 (2006).
[14] A. K. Engel, P. König, A. K. Kreiter, and W. Singer, Science **252**, 1177 (1991).
[15] S. R. Campbell and D. Wang, Physica D **111**, 151 (1998).
[16] M. Rosenbluh, Y. Aviad, E. Cohen, L. Khaykovich, W. Kinzel, E. Kopelowitz, P. Yoskovits, and I. Kanter, Phys. Rev. E **76**, 046207 (2007).
[17] F. M. Atay, J. Jost, and A. Wende, Phys. Rev. Lett. **92**, 144101 (2004).
[18] I. Matskiv, Y. Maistrenko, and E. Mosekilde, Physica D **199**, 45 (2004).
[19] C. Masoller and A. C. Martí, Phys. Rev. Lett. **94**, 134102 (2005).
[20] D. Topaj, W.-H. Kye, and A. Pikovsky, Phys. Rev. Lett. **87**, 074101 (2001).
[21] J. Kestler, W. Kinzel, and I. Kanter, Phys. Rev. E **76**, 035202(R) (2007).
[22] M. Golubitsky and I. Stewart, Bull. Am. Math. Soc. **43**, 305 (2006).
[23] S. Lepri, G. Giacomelli, A. Politi, and F. T. Arecchi, Physica D **70**, 235 (1993).
[24] R. Lang and K. Kobayashi, IEEE J. Quantum Electron. **16**, 347 (1980).
[25] V. Ahlers, U. Parlitz, and W. Lauterborn, Phys. Rev. E **58**, 7208 (1998).
[26] H. D. I. Abarbanel, N. F. Rulkov, and M. M. Sushchik, Phys. Rev. E **53**, 4528 (1996).
[27] S. Boccaletti, J. Kurths, G. Osipov, D. L. Valladares, and C. S. Zhou, Phys. Rep. **366**, 1 (2002).
[28] Usually $w_{j,j}=0$ because the self-feedback is already taken into account by the term weighted by λ. Only if a laser j gets no input from other lasers, then $w_{j,j}=1$ to compensate for the missing external input. (Alternatively one could increase the corresponding λ.)